Geostrophic approximation in the St. Lawrence estuary

By W. D. FORRESTER, *Atlantic Oceanographic Laboratory, Bedford Institute, Dartmouth, Nova Scotia, Canada*[1]

(Manuscript received September 16, 1968)

ABSTRACT

A 1965 survey of currents and geostrophic currents in the St. Lawrence estuary is described. An innovation employed in the survey was to moor the strings of oceanographic bottles in the cross-section and trip them simultaneously. A tidal oscillation was detected in the vertical shear of the geostrophic current as well as in the vertical shear of the axial and cross-channel current components. The observations qualitatively confirm predictions from a simple theory that is presented for geostrophic response on one- and two-layer canals. The theory suggests that the period of resonant cross-channel oscillation is an important time scale since current fluctuations of much longer periods reflect accurately in the geostrophic current, while fluctuations of shorter periods may appear as considerable distortions in the geostrophic current. From this, it is concluded that a single determination of geostrophic current may represent neither the instantaneous nor the long-term average current. The average geostrophic current over a time interval longer than the resonant period may, however, represent the average current over the same interval.

1. Introduction

A great deal of effort has been devoted to assessing current velocities by use of the geostrophic approximation. The geostrophic currents resemble the actual currents only insofar as the assumption that the Coriolis force is balanced by the horizontal pressure gradient force is valid. Because it is easier to measure density than it is to measure currents directly and because the temperature and salinity measurements are in demand for other applications as well, the geostrophic approximation is sometimes applied in areas where the basic assumptions are violated. The worst violations probably occur in coastal waters, where friction and acceleration are seldom negligible.

There are frequent examples in the St. Lawrence gulf and estuary of geostrophic currents, calculated from single sets of observations, being treated as if they represented fairly long-term average pictures of the actual currents. How long the interval of the time average was believed to be, however, has seldom been spelled out. The need to establish what meaning, if any, geostrophic currents have in such coastal waters decided the author to design an experimental survey that would show more clearly how the density field does in fact respond to the changing velocity field.

2. Background information

Reference has been made in the literature to short-term fluctuations in observed temperature and salinity in the St. Lawrence gulf and estuary (Huntsman, 1923; Gaudry, 1938; Nadeau, 1938; Lauzier & Filteau, 1948; McLellan, 1950; Lauzier, 1957*a* and 1957*b*). Some were reported as apparently having semidiurnal tidal periods. McLellan (1950) believes that many of the observed fluctuations were due to internal waves.

Two recent surveys in which an attempt was made to observe a correlation between observed current and geostrophic current are the 1962 and 1963 surveys (Fig. 1) carried out by R. W. Trites and W. I. Farquharson of the Bedford Institute. Farquharson (1966) reports on the

[1] Contribution No. 176 from The Bedford Institute.

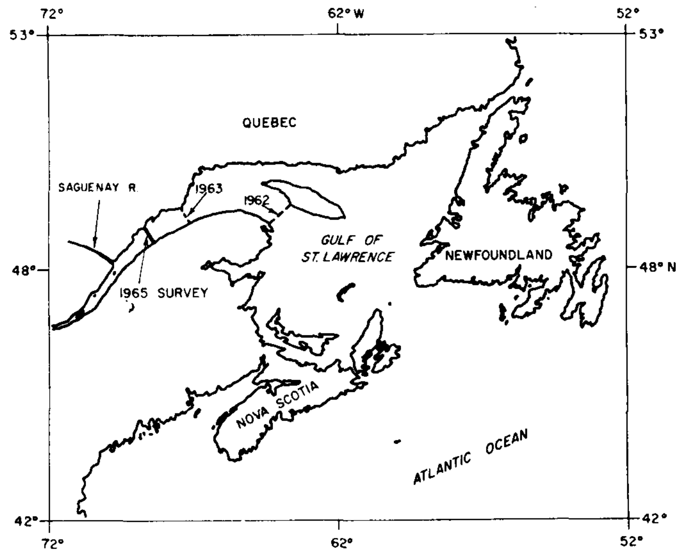

Fig. 1. Station locations, phase I and phase II.

results of the current observations from these two surveys. It was felt that failure to find correlation between geostrophic and measured currents in the 1962 data might have been caused by confusion of temporal with spatial variations in the density. Two ships were therefore used in the 1963 survey to reduce the time required to observe the section from 6 to 3 hours. Still, however, no correlation appeared between the geostrophic and measured currents.

It was apparent that if a new survey were to be more successful in relating the geostrophic current to the actual current it would be necessary to eliminate any confusion between temporal and spatial variations in the density field. This was achieved during the fall of 1965, when simultaneous sets of oceanographic observations were obtained in a section of the St. Lawrence estuary by mooring the strings of bottles and tripping them at a pre-set time by clockwork. Time series of oceanographic observations were also made at selected stations to assess the nature of the temporal changes. This paper attempts to account for relationships found between the calculated geostrophic currents and the currents measured directly by current meters on this survey.

3. Method of survey

The cross-section of the St. Lawrence estuary chosen for the survey is that shown in Figs. 1 and 2. During phase I (Sept. 16–Oct. 4) the current and oceanographic stations were located throughout the cross-section as shown in Figs. 2 and 3. The set of eight oceanographic stations (temperature and salinity) was observed once on each of 11 days. Strings of water bottles were moored on seven of the stations, and the eighth station was observed from the ship at the time for which the moored stations had been set to trip. Each mooring consisted of a subsurface float, a clockwork messenger release with depth recorder, the Knudsen water bottles, a bottom timer to record the actual time of observation, and an anchor release to permit the float to rise to the surface for recovery after the observations were completed. The time involved in setting and recovering the moorings restricted the frequency of these simultaneous observations to one set per day. During Phase I, eighteen Braincon Histogram current meters remained moored in the positions shown in Figs. 2 and 3.

During phase II (Oct. 6–Oct. 12) three strings of five current meters each were moored near the middle of the channel about a mile apart (Fig. 2). A surface marker was placed about a mile to the northwest and another about a mile to the southeast of the outer current meter strings to mark the sites on which oceanographic time series observations were to be made. These five moorings were not placed exactly in the straight line intended, but Fig. 2 shows the

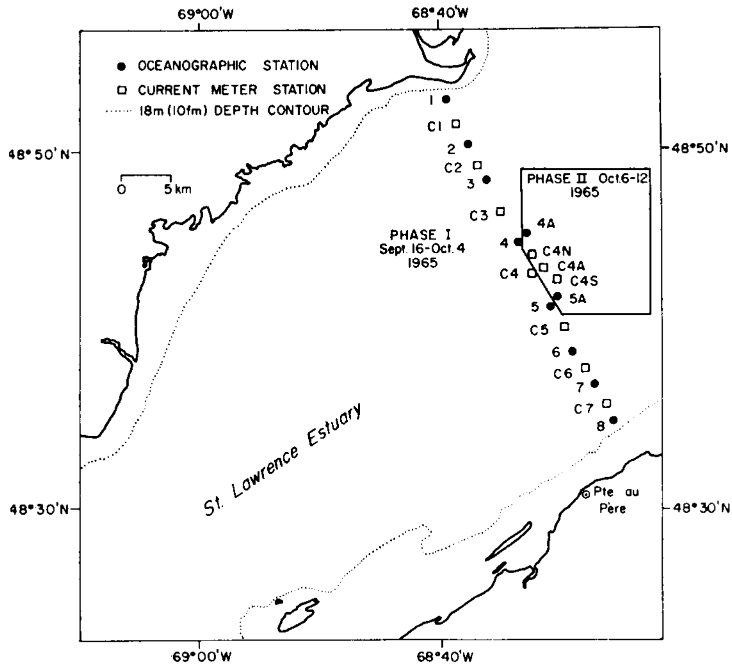

Fig. 2. General chart, showing recent surveys.

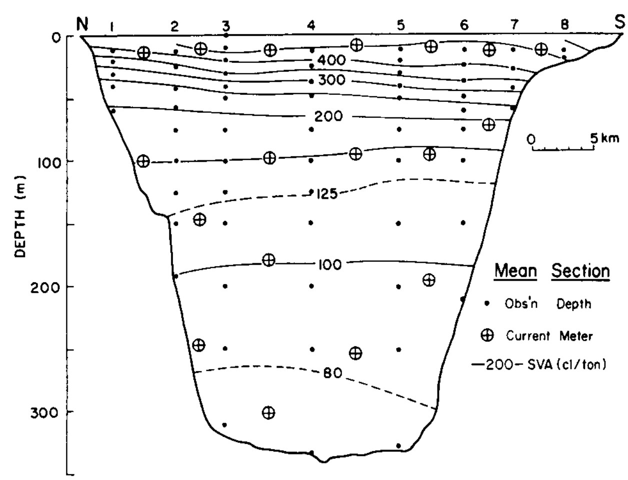

Fig. 3. Sectional plot of phase I observation depths and mean specific volume anomaly distribution.

actual positions of the moorings. The time between arrivals of the ship at successive oceanographic markers was almost exactly 1 hour, so the interval between observations at the same station was about 2 hours. Weather interrupted the time series after 24 hours, so two 24-hour series were obtained instead of the one 48-hour series. Description of the survey, mooring procedures, and instrumentation has been presented in detail by Forrester (1967).

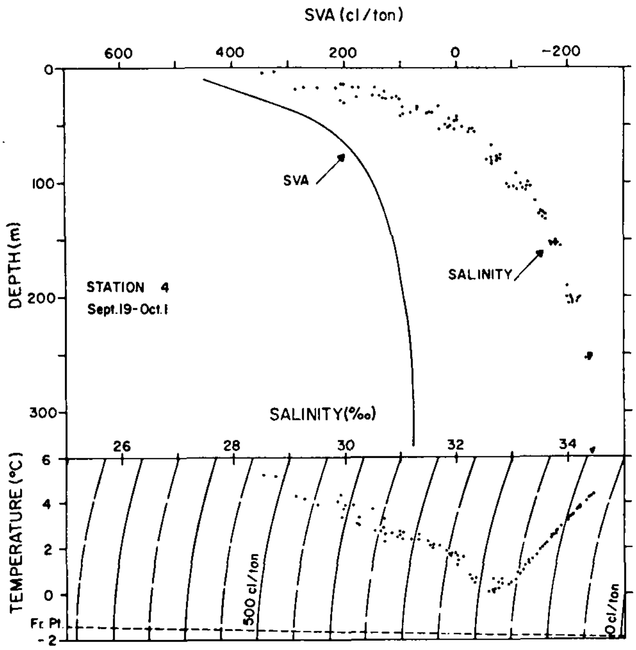

Fig. 4. Water characteristics at station 4A, phase II.

4. Quantity and quality of data

During phase I eleven of the current meters gave complete data records and seven gave no data of value. Of the 11 simultaneous oceanographic observations, two yielded sets of eight complete stations, six yielded sets of seven complete stations, and three yielded sets of six complete stations.

During phase II 10 of the 15 current meters operated satisfactorily, two operated about half the time, and three failed completely. On two of the 46 oceanographic casts the observations below 125 m were spoiled by pre-tripping; all other stations were complete.

The salinities were determined by the conductivity method, using an NIO conductivity bridge. The overall accuracy of the salinity determinations is estimated to be $\pm 0.01‰$ at the 90% confidence level. The overall accuracy of the corrected reversing thermometer readings (protected and unprotected) is estimated to be ± 0.01C° at the 90% confidence level.

The sampling depths could be more accurately determined for the moored oceanographic stations than for the ship stations. The advantages of the moored stations in this respect were (1) that the wire angles were negligibly small, and (2) that the depths of the top and bottom of the wire could both be accurately determined, the top from the pressure reading, and the bottom from the echo sounding. On both the ship and the moored stations thermometric depths were calculated for the bottles at and below 200 m. Depths adopted for the moored observations are believed accurate to ± 1 m, and those for the ship observations to the greater of ± 1 m or ± 1% of the depth.

The Braincon current meters sense current speed, current direction, and instrument tilt, all averaged over 20-minute intervals. The current speed readings were corrected for instrument tilt and resolved into components parallel to and perpendicular to the channel of the estuary. The scatter about smooth curves drawn through plots of the component speeds indicates that ± 3 cm/sec is a reasonable estimate for the accuracy of a single 20-minute determination of component speed.

5. Presentation of data

5.1 *Water characteristics*

Two composite station plots are presented here to illustrate the water characteristics in the

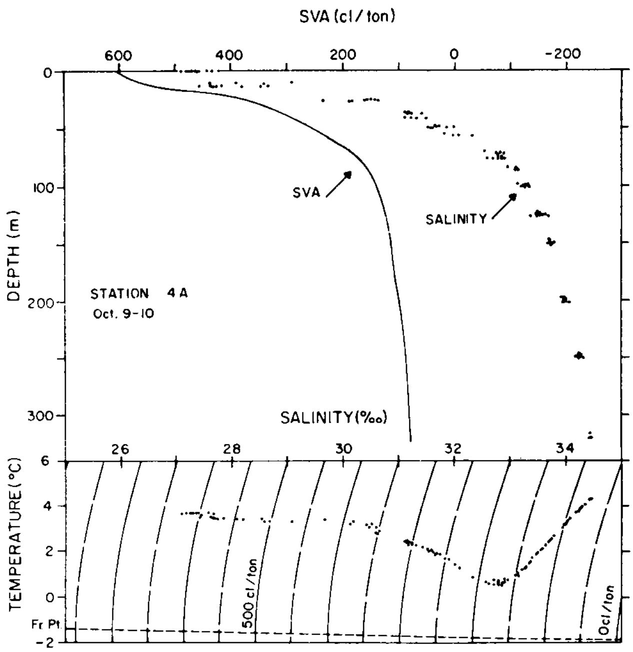

Fig. 5 Water characteristics at station 4, phase I.

estuary at the time of the survey. Fig. 4 includes all information from the 11 moorings placed at station 4 between Sept. 19 and Oct. 1, while Fig. 5 includes all information from the 12 ship occupations of station 4A between Oct. 9 and Oct. 10. The individual values are shown in the salinity *vs.* depth plots and in the temperature *vs.* salinity plots. The specific volume anomaly *vs.* depth curves are means drawn through the individual values. The scatter of the salinity points in Figs. 4 and 5 gives some indication of the changes in water characteristics occurring during a two-week and a one-day period respectively. Fig. 3 shows the mean specific volume anomaly distribution in the cross-section as determined from the 11 phase I observations. The individual sections (not shown) vary significantly from each other and from this mean section.

5.2 *Geostrophic currents*

Phase II geostrophic currents were calculated relative to the bottom (330 db) and also relative to the mean depth of the three deepest current meters (300 db). The convention that inflow through the estuary is positive is used throughout this paper. In Fig. 6 the geostrophic currents are plotted *vs.* time for each depth that a

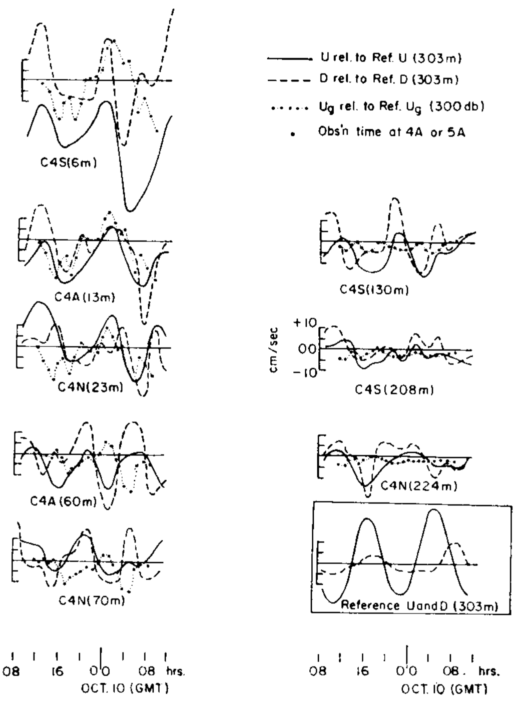

Fig. 6. Phase II geostrophic currents (U_g), axial currents (U), and cross-channel local acceleration divided by the Coriolis parameter (D), for Oct. 9 –10.

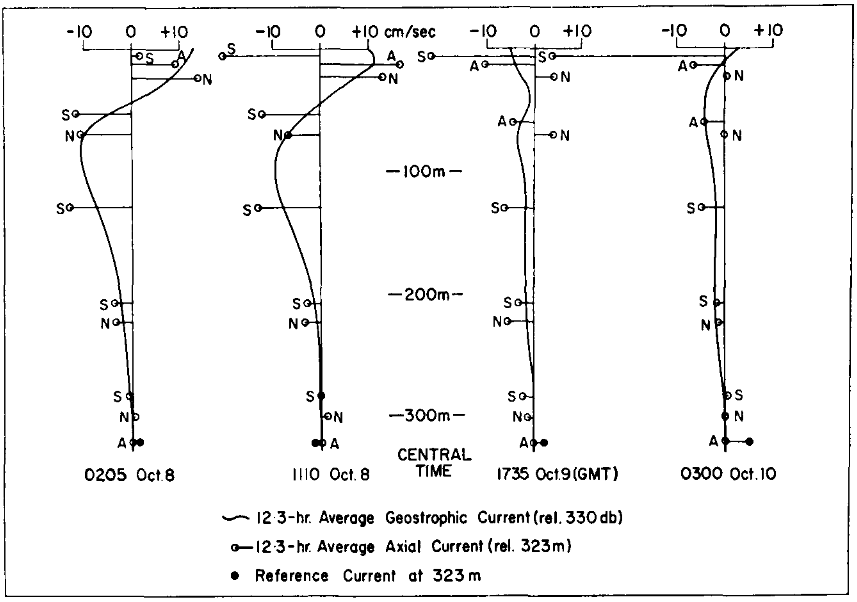

Fig. 7. Pase II geostrophic currents and axial currents averaged over M_2 tidal periods.

current meter was operating during the second half of the time series (Oct. 9–Oct. 10). Fig. 7 shows the phase II geostrophic currents averaged over M_2 tidal periods and plotted *vs.* depth.

Selection of a common reference level for the geostrophic currents of phase I was more difficult because the stations were in different depths of water. Following a method described by Montgomery (1941) the reference level was chosen as the deepest part of the channel, 330 db, and the geopotential anomaly at the bottom of each station vertical was determined by integration of the hydrostatic equation along the bottom from the 330 db level. Use of this method implies the assumption that the isobars are horizontal in the proximity of the bottom, i.e., that the geostrophic current is zero at the bottom. The phase I geostrophic currents are plotted *vs.* depth in Fig. 8. The plots are arranged in matrix fashion, with those between stations 7 and 8 in the top row, 6 and 7 in the second row, etc., and with the shore-to-shore averages (stations 1 to 8) in the bottom row. Plots for the Sept. 19 section are in the first column, Sept. 21 in the second column, etc. with plots for the mean section in the right-hand column. On most days one or more of the stations failed to trip properly. Because, for example, stations 2 and 3 were missed on Sept. 19, the plots for stations 1–2, 2–3, and 3–4 are omitted in the first column of Fig. 8, and a plot for stations 1–4 is inserted in their stead.

Fig. 9 presents evidence of an M_2 tidal constituent in the vertical shear of the geostrophic currents. The shore-to-shore geostrophic currents for the mean section were subtracted from those for the individual sections and averages then taken over the upper 50 m and over the lower 250 m. The upper layer averages relative to the corresponding lower layer averages are shown as closed circles in Fig. 9. The horizontal axis is the phase of the equilibrium tide ($E+u$ of M_2). The Sept. 19 and Oct. 1 observations have been combined because the tidal phase was the same for these two determinations. The solid curve represents a sinusoid of M_2 period fitted to the points by least squares. It has an amplitude of 9 cm/sec and a phaselag of 111° relative to the equilibrium tide.

5.3 *Current meter data*

The following expression for the cross-channel equation of motion is obtained on dividing by the Coriolis parameter and neglecting field acceleration and frictional terms:

$$U = U_g + D$$

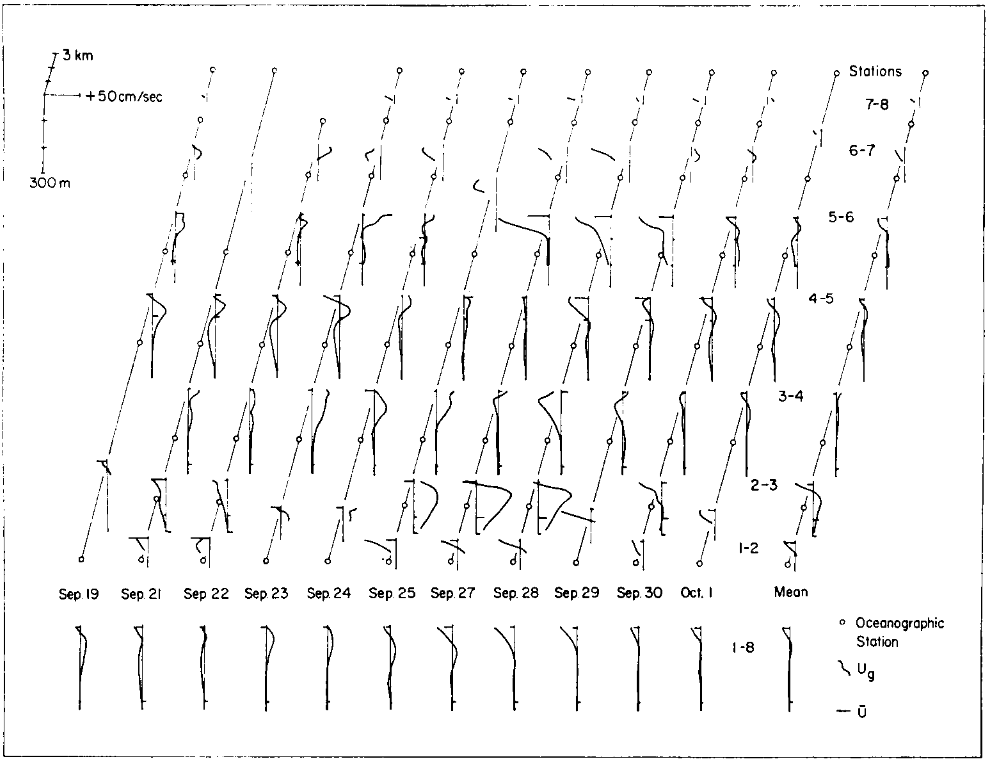

Fig. 8. Phase I geostrophic currents (U_g) and average axial currents ($\bar{U}$).

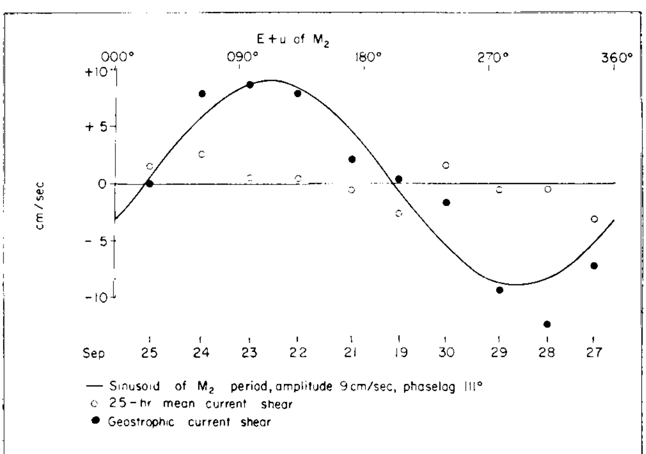

Fig. 9. Phase I geostrophic and mean axial current shears as functions of M_2 tidal phase.

in which U is the axial component of current, U_g is the axial component of geostrophic current, D is the cross-channel local acceleration divided by the Coriolis parameter.

Values of U and D are shown in Fig. 6 for each current meter in operation during Oct. 9–10. They are two-hour averages relative to the group means from the three deepest current meters.

In Fig. 7 the axial velocity components from

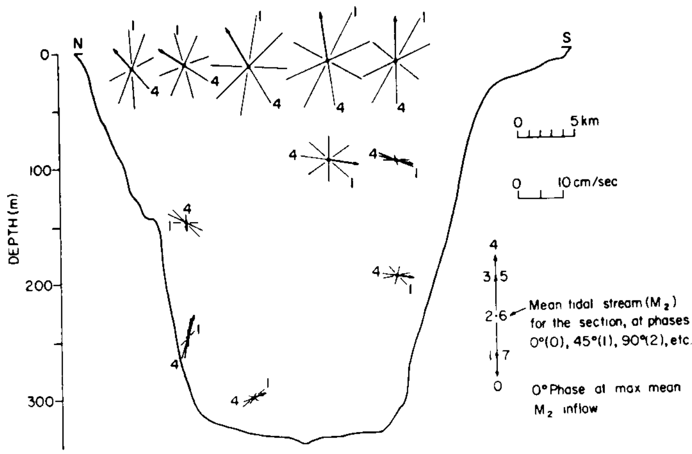

Fig. 10. Phase I local tidal streams relative to the mean tidal stream in the cross-section.

the current meters of phase II have been averaged over M_2 tidal periods and plotted relative to the corresponding value at the deepest current meter (323 m on station C4A). The reference velocity is shown as a solid circle at 323 m. The station on which the meters were moored is identified by the letter N, A, or S for stations C4N, C4A, and C4S respectively.

Averages of the phase I axial current components were formed over time intervals varying from 20 minutes to 2 weeks for comparison with the instantaneous geostrophic currents. Although none of the averages showed any significant agreement with the instantaneous geostrophic currents, a sample of the comparisons is shown in Fig. 8. The current meter values ($\bar{U}$) plotted for the individual days are averages over the 12.3 hours preceding the times of the oceanographic observations. The mean values for $\bar{U}$ in the right-hand column of Fig. 8 are averages over the entire period Sept. 19–Oct. 1.

The changes in shear between the upper and lower layer geostrophic currents of phase I have been interpreted as being related to the M_2 tidal phase at the time of the observations. To demonstratate that these are not instead related to the day-to-day changes in mean current shear, the 25-hour average current shear between upper and lower layers has been estimated from the current meter data. The five shallowest current meters were taken to represent the upper layer and the six deepest current meters to represent the lower layer. The averages cover two M_2 tidal periods and are centred at the times of the oceanographic observations. The open circles in Fig. 9 represent these 25-hour average current shears relative to the mean shear over the eleven days of observation.

5.4 *Tidal streams*

Fifteen-day harmonic analyses for tidal constituents were carried out on both the axial and cross-channel current components from the 11 meters that operated for the full period of phase I. The only tidal constituent that is considered here is the M_2 constituent. The next largest constituent, S_2, has an amplitude only about a quarter that of M_2. The M_2 constituent in the mean axial flow through the cross-section was found to have an amplitude of 12 cm/sec and a phaselag relative to the equilibrium tide of 020° (for Atlantic Standard Time). The M_2 constituent in the mean cross-channel flow was found to have an amplitude of 2 cm/sec and a phaselag of 245°.

A pronounced shear was detected between the upper and lower layers in both the axial and cross-channel tidal streams. An attempt is made to illustrate this in Fig. 10. For the purpose of locating the current meters in the cross-section, the vertical represents depth and the horizontal represents width, with the north shore on the left. For the purpose of indicating the direction of flow, the horizontal represents flow in the cross-channel direction, but the vertical represents flow in the axial direction, inflow being downward. The vectors radiating out from the current meter locations represent the local tidal streams relative to the mean tidal stream in the cross-section. These are shown at phase intervals of 45° throughout the M_2 tidal period. In the lower right-hand corner of Fig. 10 is shown the mean tidal stream to which the others have been referred. The vector mean of the axial M_2 constituents from the upper five current meters relative to that from the lower six current meters has an amplitude of 10 cm/sec and a phaselag of 247°. The vector mean of the M_2 constituents of cross-channel flow from the upper five current meters has an amplitude of 7 cm/sec and phaselag of 320°, while that from the lower six current meters has an amplitude of 3 cm/sec and a phaselag of 198°.

6. Discussion of data

6.1. *Water characteristics*

No evidence of a homogeneous upper layer deeper than 5 or 10 m appeared in any of the data. From Figs. 3, 4 and 5 it is seen to be possible, however, to define an upper and a lower layer on the basis of the rate of change of properties with depth. In the upper layer the salinity and the density increase rapidly with depth, whereas in the lower layer they increase only gradually with depth. The temperature decreases rapidly with depth in the upper layer, reaches a minimum of about 0°C near 75 m, and then increases gradually again in the lower layer. The upper layer is subject to considerable seasonal variation, and during late winter and spring takes the form of a cold homogeneous layer about 75 m thick (Forrester, 1964). The lower layer is very uniform the year round.

6.2 *Currents and geostrophic currents*

The results from phase I (Fig. 8) show that the geostrophic current pattern can change drastically over a period of a day, not only in its detail between stations, but also in its shore-to-shore value. The results from phase II (Fig. 6) indicate that appreciable changes in the geostrophic current, U_g, can occur in as little as 2 hours. These short-period fluctuations in U_g are not, however, accurate reflections of the short-period fluctuations in the current, U. At least a partial explanation for this is that the local acceleration term, D, is not negligible, as is also illustrated in Fig. 6. From the above it is clear that geostrophic current shear calculated from a single set of observations should not here be expected to represent either the instantaneous or the long-term average current shear. Furthermore, if the observations in the cross-section are not completed in less than 2 hours, a considerably distorted picture of geostrophic current could be obtained.

It may, however, still be feasible to relate the mean of several determinations of the geostrophic current to the average current over the same period, provided that this period is long enough to make the average acceleration negligible. The geostrophic profiles for the mean section of phase I (Fig. 8) fit fairly well with the current meter averages over the same period. The phase II geostrophic current profiles averaged over M_2 tidal periods (Fig. 7) also fit reasonably well with the corresponding current meter averages, except near the surface. Part of the disagreement seems due to the fact that the individual current meters do not measure the average current between the oceanographic stations. This is suggested by Fig. 7 in that currents from station C4N lie mostly to the right of the geostrophic profile, while those from C4S lie mostly to the left. Wind stress (friction) and field acceleration must also play a large part in the discrepancy between geostrophic and current meter values near the surface.

6.3 *Tidal streams and geostrophic currents*

Fig. 9 presents evidence of a tidal constituent in the geostrophic current shear between upper and lower layers. The poor correlation between the geostrophic current shear and the 25-hour average current shear, and the good correlation between geostrophic shear and tidal phase support the contention that the oscillation is properly identified as tidal. Fig. 10 demonstrates that there is also a tidal constituent in both the axial and cross-channel current shear between upper and lower layers. The tidal oscillation in the geostrophic shear is not, however, an accurate reflection of the tidal oscillation in the axial current shear; in fact, the two have nearly opposite phase.

A simple theory is presented below to predict at least qualitatively the relationship to be expected (1) between geostrophic current, cross-channel current, and an oscillating axial flow in a one-layer canal, and (2) between geo-

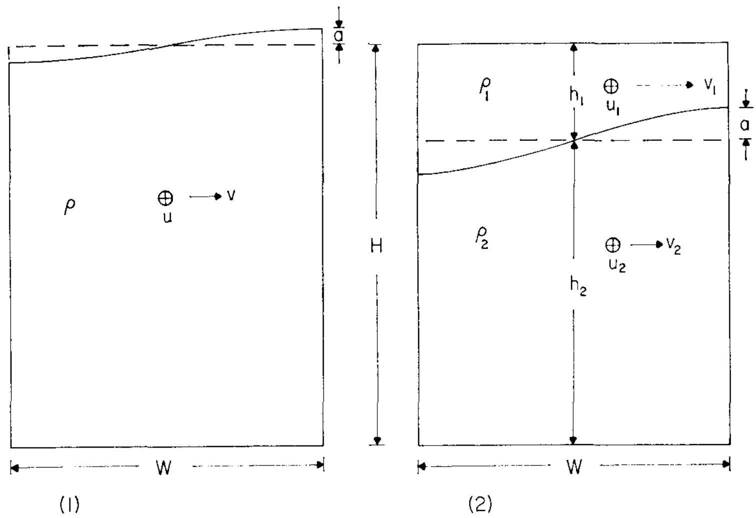

Fig. 11. (1) One-layer and (2) two-layer canals of rectangular cross-section.

strophic current shear, cross-channel current shear, and an oscillating axial shear flow in a two-layer canal.

7. Geostrophic response in canals

7.1 *One-layer canal*

Consider the cross-section of a canal (Fig. 11 (1)) through which there is an oscillating axial flow (u), uniform from top to bottom, and given as

$$u = u' \cos \omega t$$

where u' is the amplitude of the oscillation,
ω is the angular frequency of the oscillation,
t is the time, the base being chosen to give zero phaselag.

If we assume the cross-channel surface shape to be sinusoidal with a node at mid-channel and a half wavelength from shore to shore, then the geostrophic current (u_g) at mid-channel, due to the surface slope, is

$$u_g = \frac{\pi \alpha g}{f W} \tag{1}$$

where f is the Coriolis parameter,
g is the acceleration due to gravity,
W is the canal width,
α is the vertical displacement of the surface from its undisturbed height at the shore.

If v is the cross-channel flow at mid-channel and H is the undisturbed canal depth, then by continuity

$$vH = \frac{W}{\pi} \frac{d\alpha}{dt} \tag{2}$$

Thus, from (1) and (2),

$$v = \frac{f W^2}{\pi^2 g H} \frac{d}{dt}(u_g) \tag{3}$$

The resonant frequency for a cross-channel surface oscillation is

$$\omega_N = \frac{\pi \sqrt{gH}}{W} \tag{4}$$

Hence, from (3) and (4),

$$v = \frac{f}{\omega_N^2} \frac{d}{dt}(u_g) \tag{5}$$

Neglecting field acceleration and friction terms, the appropriate cross-channel equation of motion at mid-channel is

$$\frac{dv}{dt} + f u_g = f u' \cos \omega t \tag{6}$$

From (5) and (6), therefore

$$\frac{d^2}{dt^2}(u_g) + \omega_N^2 u_g = \omega_N^2 u' \cos \omega t \qquad (7)$$

(7) is the equation for undamped, forced, simple harmonic motion, and the solution is

$$u_g = \left(\frac{\omega_N^2}{\omega_N^2 - \omega^2}\right) u' \cos \omega t \qquad (8)$$

From (5) and (8), the corresponding solution for v is

$$v = \left(\frac{f\omega}{\omega_N^2 - \omega^2}\right) u' \cos\left(\omega t - \frac{3\pi}{2}\right) \qquad (9)$$

For the particular case of tidal streams in this cross-section of the St. Lawrence estuary, we may supply the following approximate values:

ω_N = 1 cycle in 00.1 hours,
f = 1 cycle in 16.0 hours,
ω = 1 cycle in 12. 3 hours (M_2 tidal frequency),

whence substitution in (8) and (9) yields

$$u_g = 1.00\, u' \cos \omega t$$

$$v = 0.00\, u' \cos\left(\omega t - \frac{3\pi}{2}\right) \qquad (10)$$

(10) predicts that in this section of the St. Lawrence estuary we should expect to find a barotropic component of geostrophic current (that due to surface slope) equal in phase and amplitude to the mean M_2 axial tidal stream, with no measurable mean cross-channel M_2 tidal stream. The observations of this survey and of earlier ones conducted by W. I. Farquharson of the Bedford Institute (Forrester, 1967) confirm the accuracy of these predictions.

7.2 *Two-layer canal*

Consider now the cross-section of a canal (Fig. 11 (2)) in which the water is stratified into two layers, with an oscillating axial flow of u_1 in the upper layer and of u_2 in the lower layer, such that

$$u_1 - u_2 = u'' \cos \omega t \qquad (11)$$

If we impose the restrictions that ω and f are both much smaller than ω_N (which is true for tidal oscillations in the estuary), the relations (10) apply. We may thus assume that the geostrophic current in the upper layer (u_{g1}), which is due to surface slope alone, is given by

$$u_{g1} = \frac{(u_1 h_1 + u_2 h_2}{H} \qquad (12)$$

and that the average cross-channel streams have zero amplitude, so that

$$v_1 h_1 + v_2 h_2 = 0 \qquad (13)$$

where h_1 is the undisturbed upper layer thickness,
h_2 is the undisturbed lower layer thickness,
H is the total depth $(h_1 + h_2)$,
v_1 is the upper cross-channel stream at mid-channel,
v_2 is the lower cross-channel stream at mid-channel.

The difference between the geostrophic current in the lower and upper layer, $u_{g1} - u_{g2}$, results from the slope of the interface between the layers, and an argument analogous to that for the one-layer canal, along with the use of (13), yields

$$u_{g1} - u_{g2} = \left(\frac{\omega_n^2}{\omega_n^2 - \omega^2}\right) u'' \cos \omega t,$$

$$v_1 = \frac{h_2}{H}\left(\frac{f\omega}{\omega_n^2 - \omega^2}\right) u'' \cos\left(\omega t - \frac{3\pi}{2}\right), \qquad (14)$$

$$v_2 = \frac{h_1}{H}\left(\frac{f\omega}{\omega_n^2 - \omega^2}\right) u'' \cos\left(\omega t - \frac{\pi}{2}\right),$$

in which ω_n is the resonant frequency for internal cross-channel oscillation of the interface, given by

$$\omega_n = \frac{\pi}{W}\sqrt{\frac{g h_1 h_2 (\varrho_2 - \varrho_1)}{H \varrho_2}},$$

where ϱ_1 and ϱ_2 are the upper and lower layer densities respectively.

7.3 *Comparison of theory and observation*

As described earlier, M_2 tidal constituents were detected in the observed vertical shear of geostrophic current, axial current, and cross-

Table 1. *Predicted and observed tidal constituents corresponding to the observed constituent $u_1 - u_2 = 10 \cos(\omega t - 247°)$ cm/sec*

	Prediction	Observation
v_1	$10 \cos(\omega t - 337°)$	$7 \cos(\omega t - 320°)$ cm/sec
v_2	$2 \cos(\omega t - 157°)$	$3 \cos(\omega t - 198°)$ cm/sec
$u_{g1} - u_{g2}$	$6 \cos(\omega t - 067°)$	$9 \cos(\omega t - 111°)$ cm/sec

channel current. If the observed shear between upper and lower layer axial tidal steams is substituted into (14), predictions are obtained for the corresponding tidal consituents in the geostrophic current shear and in the upper and lower layer cross-channel streams. Table I gives these predicted values alongside the observed values. To be consistent with the mathematical notation, the phase of the equilibrium tide ($E + u$ of M_2) is denoted as ωt. For the purpose of the predictions, the cross-section of the estuary has been treated as consisting of an upper layer 50 m thick with density 1.024 gm/cc, and a lower layer 250 m thick with density 1.027 gm/cc, which gives ω_n a value of one cycle in 20.3 hours.

It is considered that the agreement evidenced in Table I is sufficient to demonstrate the ability of the simple theory presented for one- and two-layer canals to explain, qualitatively at least, the nature of geostrophic response in such systems.

The observed shear between the M_2 tidal constituent of axial flow in the upper and lower layers ($u_1 - u_2$) has been treated here as a given quantity. It is believed to be associated with a standing internal wave of M_2 period along the axis of the estuary and tied to the abrupt shallowing of the estuary channel near the mouth of the Saguenay River (Forrester, 1967).

7.4 *Implications of theory*

It is apparent from equation (14) that the resonant period of an internal cross-channel oscillation is a pertinent time scale to consider in planning observations of geostrophic current. Oscillations in real current shear with much longer period than this might be expected to reflect almost directly in the geostrophic current shear; oscillations with period shorter than this might be expected to reflect as out-of-phase oscillations in the geostrophic current shear. The amplitude of the geostrophic response to an oscillation in current shear should be greatest when the period of oscillation equals the internal resonant cross-channel period, and should be negligibly small when the period of oscillation is much shorter than the resonant period. The appropriate cross-channel period to consider may not, of course, be that just for the simple two-layer system.

From the theory it thus follows that if there are significant fluctuations superimposed on the long-term average current shear, the geostrophic current shear determined from a single set of observations may represent neither the instantaneous nor the long-term average current shear. Further, if the time occupied in securing the set of observations were comparable with the time scale of the fluctuations a completely distorted picture of the geostrophic current would be obtained. If, however, the observations were taken in such a manner that the effects of the fluctuations were averaged out, the mean geostrophic current could accurately represent the mean real current shear over the same time interval. The time interval over which the geostrophic current is averaged should be long compared to the internal resonant cross-channel period. These implications from the simple theory are consistent with the conclusions previously reached from examination of the current and geostrophic current observations.

8. Summary

The innovation of mooring oceanographic bottles to obtain simultaneous observations proved valuable in providing information on the nature of geostrophic response in coastal channels. Because, however, only one such set of simultaneous observations could be obtained per day, it was necessary to use time series observations on two closely-spaced stations to study short-term fluctuations in geostrophic current. The results demonstrate that the density field, and hence the geostrophic currents, in the St. Lawrence estuary can change significantly in as little as two hours. These rapid changes in geostrophic current are not, however, accurate reproductions of corresponding fluctuations in the current. Thus, a single determination of geostrophic current may be representative of neither the instantaneous nor the long-

term average current. The average of several geostrophic determinations spanning a sufficiently long time interval does, however, fairly accurately reproduce the average current over the same time interval.

A simple theory presented for one- and two-layer canals predicts that current oscillations of periods much longer than the resonant period of cross-channel oscillation would reflect accurately in the instantaneous geostrophic current; that oscillations of period shorter than the resonant period would reflect as out-of-phase oscillations with distorted amplitudes; that oscillations with period nearly equal to the resonant period would reflect in the geostrophic current with greatly exaggerated amplitude; and that oscillations in the current with period much shorter than the resonant cross-channel period would reflect scarcely at all in the instantaneous geostrophic current. The implications of the theory are consistent with conclusions drawn from the observed currents and geostrophic currents. In particular, observed M_2 tidal constituents in the vertical shear of the axial and cross-channel currents and of the geostrophic currents fit well with predictions from the theory.

Acknowledgements

This work was performed with the facilities and support of the Bedford Institute, and constituted the main basis for a doctoral dissertation presented to The Johns Hopkins University in 1967. The author wishes to thank Dr. R. B. Montgomery and Dr. D. W. Pritchard of The Johns Hopkins University for their assistance and encouragement throughout the project, and Dr. C. D. Maunsell and Dr. R. W. Trites of the Bedford Institute for their valuable suggestions during the preparation of this paper.

REFERENCES

Farquharson, W. I. 1966. St. Lawrence estuary current surveys. *Bed. Inst. Oceanogr.*, Dartmouth, N, S., Can. Unpubl. man rep. 66–6.

Forrester, W. D., 1964. A quantitative temperature-salinity study of the Gulf of St. Lawrence, *Bed. Inst. Oceanogr.*, Dartmouth, N.S., Can. Unpubl. man rep. 64–11.

— 1967. Currents and geostrophic currents in the St. Lawrence estuary. *Bed. Inst. Oceanogr.*, Dartmouth, N. S., Can. Unpubl. man rep. 67–5.

Gaudry R. 1938. Les températures de l'estuaire du St.-Laurent. *Université Laval*, Québec, Can. Contr. de la Station biologique du St.-Laurent, no. 11.

Huntsman, A. G. 1923. The influence of tidal oscillations on vertical circulation in estuaries. *Trans. Roy. Soc. Can.*, vol. XVII, section V.

Lauzier, L. 1957*a*. Variations of temperature and salinity in shallow waters of the southwestern Gulf of St. Lawrence. *Fish. Res. Bd. Can. Bull.*, no. 111.

— 1957*b*. Hydrographic features of the waters of the Bay of Islands, Newfoundland, in the autumn, *Fish. Res. Bd. Can. Bull.*, no. 111.

— and Filteau, G. 1948. Observations de température et de salinité à la station Laval 290, en 1946. *Université Laval.*, Québec, Can. Rapp. gén. de la Station biologique du St.-Laurent pour l'année 1946.

McLellan, H. J. 1950. Short term fluctuations in the vertical water structure of the Gulf of St. Lawrence. *Fish. Res. Bd. Can.*, Biological Station, St. Andrews, N.B., Can. Unpubl. man rep. no. 409.

Montgomery, R. B. 1941. Transport of the Florida current off Habana. *Journal Marine Res. IV* (3).

Nadeau, A. 1938. Salinité de l'eau de l'estuaire du St.-Laurent. Université Laval, Québec, Can. de la Station biologique du St.-Laurent, no. 13.

ГЕОСТРОФИЧЕСКАЯ АППРОКСИМАЦИЯ В УСТЬЕ РЕКИ СВ. ЛАВРЕНТИЯ

Описана съемка обычных и геострофических течений в устье реки Св. Лаврентия в 1965 г. При съемке использовалась сеть гидрологических станций с батометрами в поперечном разрезе реки. Приливные колебания обнаруживаются в вертикальном сдвиге геострофического течения так же, как и в вертикальном сдвиге осевой и поперечной течению компоненты. Наблюдения качественно подтверждают выводы простейшей теории геострофического течения в одно- и двухслойной моделях. Теория предполагает, что период резонансных поперечных колебаний является характерным масштабом, так как колебания больших периодов хорошо описываются геострофической моделью, тогда как колебания меньших периодов, по-видимому, сильно искажаются в геострофической модели. Из этого можно заключить, что единичное определение геострофического течения не может представлять ни мгновенного, ни среднего за долгий срок течения. Однако, геострофическое течение, осредненное за время, большее, чем период резонанса, может давать среднее течение за тот же период.